Mathematics Faculty Publications                    Mathematics and Statistics Department

# Viscosity of Bacterial Suspensions: Hydrodynamic Interactions and Self-induced Noise

Shawn D. Ryan
*Cleveland State University*, s.d.ryan@csuohio.edu

Brian M. Haines
*Pennsylvania State University*

Leonid Berlyand
*Pennsylvania State University*

Falko Ziebert
*UMR CNRS*

Igor S. Aranson
*Argonne National Laboratory*

# Viscosity of bacterial suspensions: Hydrodynamic interactions and self-induced noise

Shawn D. Ryan,[1,2] Brian M. Haines,[1,2] Leonid Berlyand,[1] Falko Ziebert,[3] and Igor S. Aranson[2]

[1]*Department of Mathematics, Pennsylvania State University, University Park, Pennsylvania 16802, USA*
[2]*Materials Science Division, Argonne National Laboratory, 9700 S. Cass Avenue, Argonne, Illinois 60439, USA*
[3]*Laboratoire de Physico-Chimie Théorique, UMR CNRS Gulliver 7083, ESPCI, 10 rue Vauquelin, F-75231 Paris, France*

The viscosity of a suspension of swimming bacteria is investigated analytically and numerically. We propose a simple model that allows for efficient computation for a large number of bacteria. Our calculations show that long-range hydrodynamic interactions, intrinsic to self-locomoting objects in a viscous fluid, result in a dramatic reduction of the effective viscosity. In agreement with experiments on suspensions of *Bacillus subtilis*, we show that the viscosity reduction is related to the onset of large-scale collective motion due to interactions between the swimmers. The simulations reveal that the viscosity reduction occurs only for relatively low concentrations of swimmers: Further increases of the concentration yield an increase of the viscosity. We derive an explicit asymptotic formula for the effective viscosity in terms of known physical parameters and show that hydrodynamic interactions are manifested as self-induced noise in the absence of any explicit stochasticity in the system.

Collective dynamics of self-locomoting micro-organisms, such as bacteria, algae, and sperm cells [1–6], as well as synthetic swimmers [7,8], have attracted enormous attention, with a large number of experimental and theoretical works published in the past few years. A plethora of nontrivial properties have been predicted and consequently studied, including dynamic instabilities, anomalous density fluctuations, nontrivial stress-strain relations, rectification of chaotic motion, and viscosity reduction [9–15]. A sevenfold viscosity reduction in a suspension of swimming bacteria, *Bacillus subtilis*, was observed recently in Ref. [16]. Such a dramatic effect occurred in the regime of well-developed large-scale collective motion of the bacteria above a certain critical concentration, about 1–2% of volume fraction; for larger filling fractions (about 6–10%), the viscosity increased, as would be anticipated for passive suspensions.

Reference [11] was the first to consider the effects of self-propulsion on the viscosity of active suspensions. While very stimulating for its time, in Ref. [11] pure relaxational dynamics of the alignment was assumed, whereas in planar shear flow individual swimmers perform periodic rotations (Jeffery orbits). The viscosity reduction for dilute suspensions (i.e., for negligible interactions between the swimmers) has been addressed in a number of theoretical works [17–20]. Reference [17] first demonstrated the necessity of rotational noise in order to produce a reduction in the effective viscosity for a suspension in flows with vorticity. The analysis led to rather counterintuitive conclusions: For planar shear flow the viscosity reduction occurs only if swimmers undergo rotational diffusion (e.g., tumbling). Without tumbling, the net contribution to the viscosity of noninteracting swimmers is zero [17,19]! In apparent contradiction to this, a viscosity reduction has been measured without noticeable tumbling (for most experimental conditions) for *Bacillus subtilis* [3,16].

In this Rapid Communication we investigate, numerically and analytically, the influence of hydrodynamic interactions on the effective viscosity of a three-dimensional suspension of swimming bacteria. We demonstrate that hydrodynamic interbacterial interactions have a similar effect on the effective

viscosity as rotational diffusion or tumbling have in the dilute case (no interactions) [17]. Both simulations and analytical theory reveal that the viscosity reduction occurs due to hydrodynamic interactions between the swimmers, and no tumbling is needed. The bacteria are modeled by massless self-locomoting point dipoles suspended in a viscous fluid. Simulations show that as the concentration increases, the viscosity initially decreases and then increases (Fig. 1), which is in qualitative agreement with recent experiments. We further analyzed the hydrodynamic interactions in the continuum limit and show that viscosity reduction is associated with the breakdown of the uniform state in concentration.

*Model.* Bacteria are modeled by massless hydrodynamic point dipoles of strength $U_0 \sim V_0 l^2$ (stresslets normalized by the solvent viscosity $\eta_0$) swimming with speed $V_0$ with respect to the fluid along the orientation of its dipole moment $\mathbf{d}_i$, where $i = 1, \ldots, N$, $N$ being the number of bacteria and $l$ is the characteristic size of a bacterium. We scale the velocities by the bacterium's swimming speed $V_0 \sim 20\ \mu$m/s, the positions by the characteristic size $l = 1\ \mu$m, the dipole strength by $l^2$; the unit of time is 1/20 s. The positions $\mathbf{r}_i$ and orientations $\mathbf{d}_i$ of the bacteria are governed by

$$\frac{d\mathbf{r}_i}{dt} = V_0\mathbf{d}_i + \sum_{j \neq i}(\mathbf{v}_{ij} + \mathbf{F}_{ij}) + \mathbf{V}_{\text{BG}}, \frac{d\mathbf{d}_i}{dt} = \mathbf{\Omega}_i, \quad (1)$$

where BG denotes the background flow and $\mathbf{\Omega}_i$ is the rotation rate for $i$th dipole. $\mathbf{v}_{ij}$ is the fluid velocity field produced by the $j$th bacterium on the $i$th and is the solution to Stokes equation at $|\mathbf{r}_j - \mathbf{r}_i|$ for a point dipole at the origin with orientation $\mathbf{d}_j$. We consider planar shear flow in the $x - y$ plane, hence $\mathbf{V}_{\text{BG}}$ is given by $V_y = \dot{\gamma}x$, $V_x = V_z = 0$; $\dot{\gamma}$ is the strain rate. The rotation rate is expressed via the vorticity $\omega_j = (\nabla \times \mathbf{v}_{ij})$ and rate of strain tensor $\hat{\mathbf{E}}_j = (1/2)(\nabla\mathbf{v}_{ij} + \nabla\mathbf{v}_{ij}^T)$ of the flow. $\mathbf{\Omega}_i = -\mathbf{d}_i \times [\omega_{\text{BG}} + \sum_{j \neq i}\omega_j + B_0\mathbf{d}_i \times (\mathbf{E}_{\text{BG}} + \sum_{j \neq i}\hat{\mathbf{E}}_j) \cdot \mathbf{d}_i]$, where $B_0$ is the Bretherton constant ($B_0 = 0/1$ for spheres/needles) [21]. The hydrodynamic interactions are contained in $\mathbf{v}_{ij}, \mathbf{\Omega}_i$ (see Ref. [22]). $\mathbf{F}_{ij} = -\partial L_{ij}/\partial \mathbf{r}_{ij}$ in Eq. (1) is a short-range repulsive force modeled by a Lennard-Jones-type (LJ) potential,
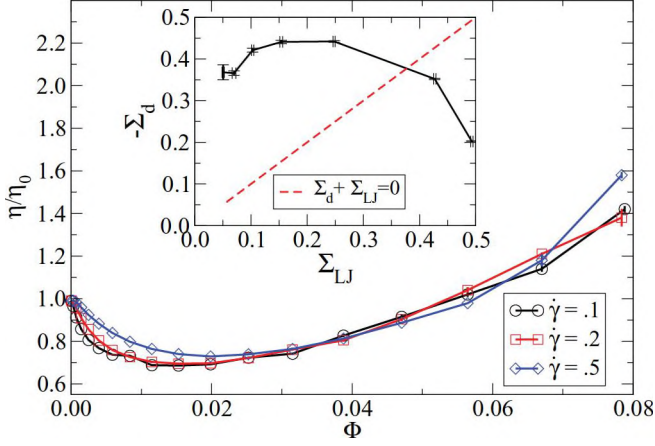
FIG. 1. (Color online) Viscosity $\eta$ vs. filling fraction $\Phi$ for pushers for three strain rates $\dot{\gamma}$. $\Phi = \frac{4}{3}\pi\sigma_{LJ}^3\rho$, where $\rho$ is the concentration, $V_0 = 1$. (Inset) Dipolar stress $\Sigma_d$ vs. LJ stress $\Sigma_{LJ}$; $\sigma_{LJ} = .35$, $B_0 = 0.95$, and $U_0 = -8\pi V_0$ (pushers).

$L_{ij} = 4\varepsilon[(\sigma_{LJ}/r_{ij})^{12} - (\sigma_{LJ}/r_{ij})^6]$. Here $r_{ij} = |\mathbf{r}_i - \mathbf{r}_j|$ is the distance between the two particles and $\varepsilon \sim (\eta_0 l^2)^{-1}$ is the normalized strength of interaction; $\sigma_{LJ}$ determines the equilibrium distance. The role of the repulsive potential is twofold. First, short-range repulsion is needed for regularization of the dipole forces, which diverge as $1/r^2$: When bacteria approach a certain distance determined by the parameter $\sigma_{LJ}$, they are pushed away. Thus, this parameter determines indirectly the size of a bacterium and therefore introduces excluded volume constraints. Second, this potential introduces on a very simplified level additional dissipation due to inelastic collisions between bacteria and deviations from the fluid velocity field of a point dipole. A spherically symmetric LJ potential is used. Simulations where run with an anisotropic LJ potential and no qualitative difference was found. While the form of the potential is not crucial for the model, the LJ one is convenient. This approach has been justified by experiments showing the flow created by a bacterium is described by a point dipole [23]. While close-field interactions are important when considering two bacteria swimming near each other, we consider only bulk properties where these individual interactions are shown to be unimportant. The simulations were performed in a cubic domain (size $L = 50$), with periodic boundary conditions in $y$ and $z$ and Lees-Edwards conditions in the $x$ direction along the sheared boundary [24]. Simulations of up to $N = 48^3$ particles were implemented on graphic processing units and performed for varying strain rates $\dot{\gamma}$, swimming speeds $V_0$, and sizes of bacteria $\sigma_{LJ}$.

Select results for viscosity $\eta$ vs. volume fraction of bacteria $\Phi$ are shown in Fig. 1. The viscosity is defined as $\eta = \eta_0(1 + \Sigma_{xy}/\dot{\gamma})$, where $\Sigma_{l,m}$ is the stress tensor,

$$\Sigma_{l,m} = \sum_{i=1}^{N}\left[\frac{U_0}{V_L}\left(d_i^{(m)}d_i^{(l)} - \frac{\delta_{lm}}{3}\right) + \frac{r_i^{(m)}F_i^{(l)}}{V_L}\right]. \quad (2)$$

The first term is due to the dipolar contribution $\Sigma_d$ [25], and the last term is due to the LJ forces between bacteria $\Sigma_{LJ}$ [26]; $V_L = L^3$ is the volume of the integration domain. For $U_0 < 0$ (pushers), the viscosity decreases with increasing filling

fraction $\Phi$; see Fig. 1. Then, for high filling fractions, two simultaneous trends occur: (i) the last term in Eq. (2) increases leading to the viscosity increase; (ii) due to the increased concentration, collisions become increasingly frequent and alter the orientations of the bacteria leading to a saturation of the contribution from $\Sigma_d$ in Eq. (2).

The inset to Fig. 1 illustrates the relationship between stresses $\Sigma_d, \Sigma_{LJ}$ for varying swimming speeds, $V_0$ and $\Phi = 0.02$. When the collisional stress $\Sigma_{LJ}$ increases, the orientational order (characterized by $\Sigma_d$) decreases. Thus, the increase in viscosity in Fig. 1 is not caused solely by the increased concentration but also by the disruption of orientation due to the collisions. In Fig. 1 the increase in viscosity for a fixed swimming speed, $V_0 = 1.0$, begins where volume fractions are between 2 and 6%. For pullers ($U_0 > 0$) we always observed an increase of the viscosity with concentration; see the inset of Fig. 2. The viscosity appears to increase with increasing strain rate $\dot{\gamma}$ (shear thickening). Figure 1 shows that for small $\Phi$ with an increase of $\dot{\gamma}$, the effect of interactions diminishes (resulting in a smaller viscosity reduction). As $\Phi$ becomes larger the LJ forces become the dominant contributor to the viscosity regardless of the shear rate: The curves for differing shear rates are essentially the same. Also, in accordance with Ref. [16], as $V_0$ increases the viscosity decreases (see Fig. 2).

The distribution of bacterial orientations $P_d(\alpha, \beta)$ is shown in Fig. 3 with $\alpha, \beta$ the spherical angles of the unit vector: $d_x = \cos\alpha\sin\beta, d_y = \sin\alpha\sin\beta, d_z = \cos\beta$. As we see from Fig. 3, the maximum of the distribution shifts from ($\alpha = \pi/2, \beta = \pi/2$) to ($\alpha = \pi/4, \beta = \pi/2$) with increasing concentration. Note that a similar realignment occurs in the non-interacting case with tumbling [17]; however, for a different reason: There the transition is governed by the shear rate.

*Continuum model.* In order to obtain further insights into the role of hydrodynamic interactions we consider the continuum limit of Eq. (1). We assumed that the suspension can be described by a probability density $P(\mathbf{r}, \mathbf{d})$ of finding a bacterium with orientation $\mathbf{d}$ at location $\mathbf{r}$; $P(\mathbf{r}, \mathbf{d})$ satisfies the equation

$$\partial_t P = -\nabla_\mathbf{r} \cdot (\mathbf{V}P) - \nabla_\mathbf{d} \cdot (\Omega P), \quad (3)$$

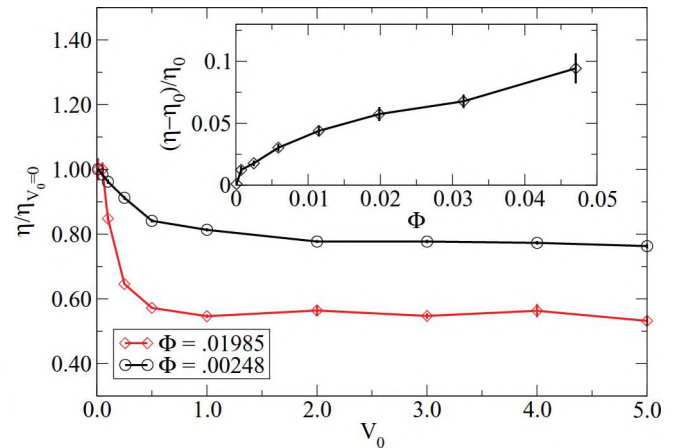FIG. 2. (Color online) $\eta$ vs. $V_0$ for $B_0 = 0.95, \sigma_{LJ} = .35$, and $U_0 = -8\pi V_0$, viscosity is scaled by $\eta$ when $V_0 = 0$. (Inset) $\eta$ vs. $\Phi$, $B_0 = 0.2$, $\sigma_{LJ} = .35$, and $U_0 = 8\pi V_0$ (pullers).
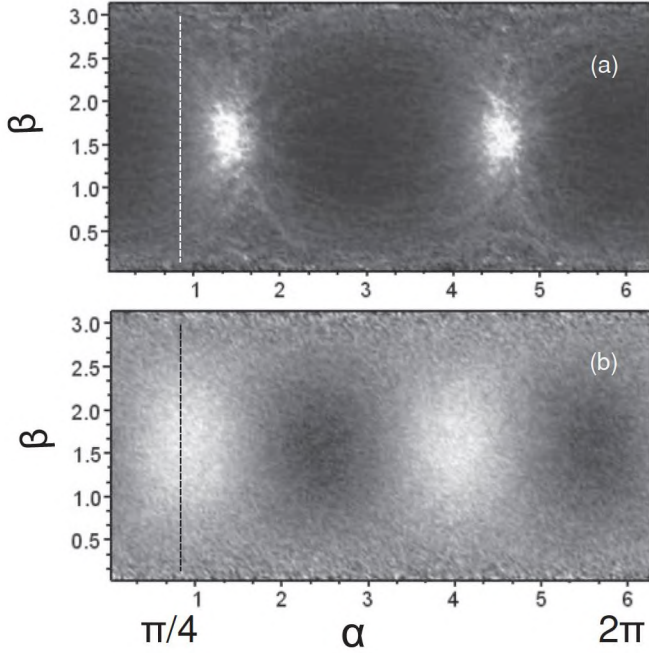
FIG. 3. $P(\alpha,\beta)$ for $\Phi = .0003$ (a) and $\Phi = .005$ (b). Vertical lines indicate $\alpha = \pi/4$; $V_0 = 1, \sigma_{LJ} = .35, U_0 = -8\pi V_0, B_0 = 0.95$. Maxima are shown in white and minima in black.

where translational $\mathbf{V}$ and rotational $\mathbf{\Omega}$ fluxes are obtained by replacing in Eq. (1) sums by integrals, $\sum_{j \neq i} A_{ij} \rightarrow V_L^{-1} \int d\mathbf{r}' d\mathbf{d}' A(\mathbf{r} - \mathbf{r}', \mathbf{d}, \mathbf{d}') P(\mathbf{r}', \mathbf{d}') + \zeta$, where $A$ is one of $\mathbf{v}, \mathbf{\Omega}, \hat{E}$, and primes denote integration variables (compare to Ref. [15]). In the derivation of Eq. (3) we neglected fluctuating terms $\zeta$ describing deviations from the mean-field approximation given by the function $P(\mathbf{r}, \mathbf{d})$. Their role will be discussed later.

The quantity of interest is the orientation distribution $P_d(\mathbf{d}) = \int d\mathbf{r} P(\mathbf{r}, \mathbf{d})/(\rho V_L)$, with $\rho = \int d\mathbf{r} d\mathbf{d} P(\mathbf{r}, \mathbf{d})/V_L$ the mean concentration. To obtain the angular distribution, we substitute $P(\mathbf{r}, \mathbf{d})$ into Eq. (3) and integrate over $\mathbf{r}$.

The resulting equation cannot be solved analytically in the general case. We thus consider the limit of small non-sphericity, $B_0 \rightarrow 0$. We assume for simplicity (the assumption is valid for $B_0 \rightarrow 0$) that $P(\mathbf{r}, \mathbf{d}) = P_r(\mathbf{r}) P_d(\mathbf{d})$, where $P_r(\mathbf{r}) = \int P d\mathbf{d} = \int d\mathbf{k} C_k \exp(i\mathbf{k}\mathbf{r})$ is the local concentration and $C_k$ its Fourier component. We can search for a steady-state solution of the form $P_d(\mathbf{d}) \approx (4\pi)^{-1}\{1 + \sin^2 \beta [A \sin(2\alpha) + B \cos(2\alpha)]\} + \dots$, where the coefficients $A, B \sim B_0$ are to be determined. These calculations were performed in the regime where $U_0 B_0 \sim O(1)$ in agreement with numerical simulations. Straightforward, but very cumbersome, calculations [22] yield the following result for the coefficients $A, B$:

$$A = -\frac{48 B_0^2 \pi^2 U_0 \rho \epsilon}{50 \dot{\gamma} R}, \quad B = -\frac{3 B_0}{2R}. \quad (4)$$

Here $\epsilon = \nu/\rho^2$ is the time-averaged normalized variance of concentration, $R = 1 + \xi^2, \xi = \frac{16\pi^2 \rho B_0 U_0 \epsilon}{25\dot{\gamma}}$ and

$$\nu = \frac{1}{V_L^2} \int d\mathbf{k} |C_k|^2 [1 - \delta(k)] = \frac{1}{V_L^2}\left[ \int d\mathbf{r} P_r^2 - \left( \int d\mathbf{r} P_r \right)^2 \right].$$

In the derivation of Eq. (4) we assumed isotropy of the positional fluctuations, i.e., that $|C_k|^2$ only depends on the modulus $|\mathbf{k}|$; the assumption is later supported by comparison with numerical simulations. Finally, we obtain the following approximate expressions for the orientation distribution $P_d$ and the viscosity $\eta$ (we neglect for simplicity the contribution due to the LJ interactions)

$$P_d(\alpha,\beta) \approx \frac{1}{4\pi} - \frac{3 B_0}{8\pi R} \sin^2 \beta \left[\cos(2\alpha) + \xi \sin(2\alpha)\right] \quad (5)$$

$$\frac{\eta}{\eta_0} - 1 = \frac{\rho U_0}{\dot{\gamma}} \int d_x d_y P_d d\mathbf{d} = -\frac{16 B_0^2 \pi^2 U_0^2 \rho^2 \epsilon}{125 \dot{\gamma}^2 R}. \quad (6)$$

One sees that for $U_0 < 0$ (pushers), the asymptotic solution as $\dot{\gamma} \rightarrow 0$ is $P_d \sim (1/\dot{\gamma}) \sin^2(\beta) \sin(2\alpha)$, i.e., has a maximum at $\alpha = \pi/4$ and $\beta = \pi/2$, in agreement with our numerical simulations. In the dilute limit ($\rho \rightarrow 0$) or in the spatially homogeneous case ($\epsilon = 0$) the distribution function $P_d \sim -\sin^2(\beta) \cos(2\alpha)$ has a maximum at $\alpha = \pi/2$ and $\beta = \pi/2$ and no viscosity reduction is seen. For $\epsilon \neq 0$ there is a viscosity reduction for pushers ($U_0 < 0$), again in agreement with our simulations and experiments [16]. Our results also hint at a relationship between collective motion and viscosity reduction: Positional fluctuations (leading to nonzero $\epsilon$) arise due to a large-scale organized motion of swimmers via an instability of the homogeneous state [15].

It is interesting to compare the expression for the viscosity (6) with the relationship obtained in Ref. [17] for the noninteracting case in the presence of tumbling (i.e., rotational diffusion with coefficient $D$). Expressions become similar for $D = -(8\pi^2 \rho B_0 U_0 \epsilon)/75 > 0$ for pushers. This suggests that hydrodynamic interactions lead, via a breakdown of the spatially homogeneous state ($\epsilon \neq 0$), to an effective rotational diffusion/tumbling.

To check our predictions given by Eq. (6) we performed simulations for small nonsphericity, $B_0 = 0.2$. Results are summarized in Fig. 4. The concentration variance $\epsilon$ was
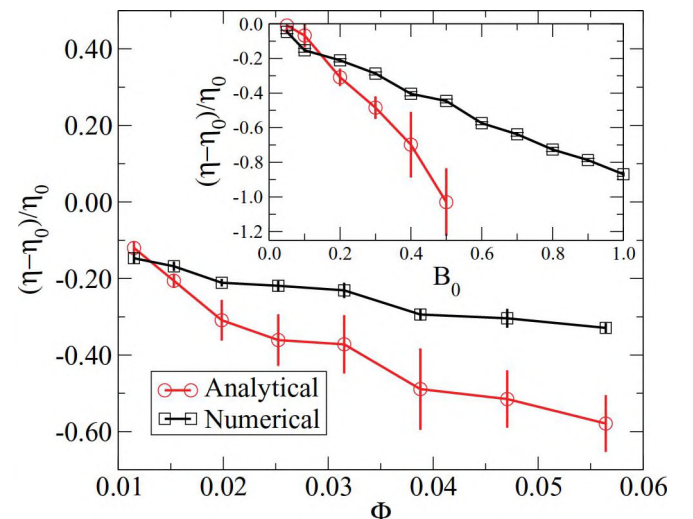


FIG. 4. (Color online) $\eta$ vs. $\Phi$, $B_0 = 0.2$, $U_0 = -8\pi V_0$. (Inset) Viscosity $\eta$ vs. Bretherton constant $B_0$ for $\Phi = .01986$. The error bars in the analytical results are due to uncertainty in the numerical calculation of the concentration variance.

extracted from the instant particle positions averaged over long periods of time on a two-dimensional square mesh in the $x - y$ plane. For simplicity we assumed that there is no $z$ dependence of the averaged concentration. This reduced significantly the statistical local density variations related to fluctuations of the number of particles, $N_i$, entering/leaving bin $i$ (the "fluctuational" variance of the number of particles $\delta N_i \sim N_i$ becomes important when there is a small number of particles in each bin). As one sees from Fig. 4, the numerical results agree with Eq. (6) within 10–15%. The inset of Fig. 4 shows that the approximation breaks down for larger $B_0$ and the theory would overestimate the decrease in viscosity. Figure 1 was plotted using $B_0 = 0.95$ for comparison with experimental observations [16]. The effect on viscosity is similar, but the magnitude decreases as $B_0 \to 0$.

Let us now discuss pullers. Experiments [27] and our simulations show an increase of viscosity, whereas Eq. (6) predicts a reduction independent of the sign of $U_0$. However, for pullers there is no instability toward collective motion [15] and thus $\epsilon = 0$. Hence fluctuations, i.e., deviations from the mean field in Eq. (3), cannot be neglected as for pushers: In a well-developed collective state the fluctuations are small compared to the mean field. The fluctuations (denoted above by $\zeta$ but then neglected) can be treated as uncorrelated noise acting on each swimmer. Simple calculations give the following estimate for the effective rotational diffusion $D_h$: $\langle \zeta(t)\zeta(t') \rangle = D_h \delta(t - t')$ and $D_h \sim \tau B_0^2 U_0^2 \rho / \sigma_{LJ}^3$. The correlation time of hydrodynamic fluctuations $\tau$ can be estimated as the time between collisions $\tau \approx 1/V_0 \rho^{1/3}$. With $U_0 \sim V_0 \sigma_{LJ}^2$ we arrive at $D_h \sim V_0 \sigma_{LJ} B_0^2 \rho^{2/3}$. Substituting $D_h$ into the expression for viscosity due to rotational diffusion [17], we obtain for pullers $\eta/\eta_0 - 1 \sim \rho U_0 D_h/(\dot{\gamma}^2 + D_h^2)$, i.e., indeed a viscosity increase in accordance with [27] and Fig. 2.

In conclusion, we have shown that the viscosity reduction as a function of concentration observed for pushers occurs primarily due to hydrodynamic interactions between swimmers. The effect of interactions on the effective viscosity is analogous to that of rotational noise in the dilute case. This effect, arising due to density fluctuations and the breakdown of the homogeneous state of the swimmers, can be interpreted as the *self-induced noise* in a system with no stochasticity. For pullers, in contrast, the homogeneous state is stable. Thus the mean-field treatment presented here yields no contribution and the behavior can be roughly described by small-scale uncorrelated fluctuations. We presented a testable prediction for the orientation distribution of interacting bacteria in sheared suspensions.

[1] X.-L. Wu and A. Libchaber, Phys. Rev. Lett. **84**, 3017 (2000).

[2] C. Dombrowski, L. Cisneros, S. Chatkaew, R. E. Goldstein, and J. O. Kessler, Phys. Rev. Lett. **93**, 098103 (2004).

[3] A. Sokolov, I. S. Aranson, J. O. Kessler, and R. E. Goldstein, Phys. Rev. Lett. **98**, 158102 (2007).

[4] I. H. Riedel, K. Kruse, and J. Howard, Science **309**, 300 (2005).

[5] J. P. Hernandez-Ortiz, C. G. Stoltz, and M. D. Graham, Phys. Rev. Lett. **95**, 204501 (2005).

[6] K. C. Leptos, J. S. Guasto, J. P. Gollub, A. I. Pesci, and R. E. Goldstein, Phys. Rev. Lett. **103**, 198103 (2009).

[7] M. Ibele, T. E. Mallouk, and A. Sen, Angew. Chem. **48**, 3308 (2009).

[8] H. Ke, S. Ye, R. Lloyd Carroll, and K. Showalter, J. Phys. Chem. A **114**, 5462 (2010).

[9] P. T. Underhill, J. P. Hernandez-Ortiz, and M. D. Graham, Phys. Rev. Lett. **100**, 248101 (2008).

[10] R. A. Simha and S. Ramaswamy, Phys. Rev. Lett. **89**, 058101 (2002).

[11] Y. Hatwalne, S. Ramaswamy, M. Rao, and R. A. Simha, Phys. Rev. Lett. **92**, 118101 (2004).

[12] H. P. Zhang, A. Beer, E.-L. Florin, and H. L. Swinney, Proc. Natl. Acad. Sci. USA **107**, 13626 (2010).

[13] A. Sokolov, M. M. Apodaca, B. A. Grzybowski, and I. S. Aranson, Proc. Natl. Acad. Sci. USA **107**, 969 (2010).

[14] I. S. Aranson, A. Sokolov, J. O. Kessler, and R. E. Goldstein, Phys. Rev. E **75**, 040901 (2007).

[15] D. Saintillan and M. J. Shelley, Phys. Rev. Lett. **99**, 058102 (2007); **100**, 178103 (2008).

[16] A. Sokolov and I. S. Aranson, Phys. Rev. Lett. **103**, 148101 (2009).

[17] B. M. Haines, A. Sokolov, I. S. Aranson, L. Berlyand, and D. A. Karpeev, Phys. Rev. E **80**, 041922 (2009).

[18] B. M. Haines, I. S. Aranson, L. V. Berlyand, and D. A. Karpeev, Phys. Biol. **5**, 046003 (2008).

[19] V. Gyrya, K. Lipnikov, I. S. Aranson, and L. V. Berlyand, J. Math. Biol. **62**, 707 (2011).

[20] D. Saintillan, Phys. Rev. E **81**, 056307 (2010); Exp. Mech. **50**, 1275 (2009).

[21] S. Kim and S. Karilla, *Microhydrodynamics: Principles and Selected Applications* (Dover, London, 2005).

[22] See supplemental information at [http://link.aps.org/supplemental/10.1103/PhysRevE.83.050904]

[23] K. Drescher *et al.* (to be published).

[24] A. W. Lees and S. F. Edwards, Journal of Physics C **5**, 1921 (1972).

[25] G. K. Batchelor, J. Fluid Mech. **41**, 545 (1970).

[26] F. Ziebert and I. S. Aranson, Phys. Rev. E **77**, 011918 (2008).

[27] S. Rafai, L. Jibuti, and P. Peyla, Phys. Rev. Lett. **104**, 098102 (2010).